Todor I. Todorov
Olivia de Carmejane
Nils G. Walter
Michael D. Morris

Department of Chemistry,
University of Michigan,
Ann Arbor, MI, USA

Capillary electrophoresis of RNA in dilute and semidilute polymer solutions

We report separations of RNA molecules (281-6583 nucleotides) by capillary electrophoresis in dilute and semidilute solutions of aqueous hydroxyethylcellulose (HEC) ether in varying buffers. RNA mobility and peak band widths are examined under both nondenaturing and also denaturing conditions. From studies of sieving polymer concentration and chain length, it is found that good separations can be obtained in semidilute solutions as well as in dilute solutions. The dependence of RNA mobility on its chain length is consistent with separation by a similar to transient entanglement mechanism in dilute solutions. In semidilute entangled solutions the separation proceeds by segmental motion.

Keywords: RNA / Capillary electrophoresis / Polymer solutions EL 4497

1 Introduction

Capillary electrophoresis (CE) is widely used for the separation of single-stranded (ss), double-stranded (ds) and supercoiled (sc) DNA, and for DNA sequencing [1]. Compared to slab-gel electrophoresis, the separation carried out in a gel-filled capillary tube has the advantage of higher resolution and sensitivity, shorter separation time, and the possibility of accurate quantification. However, a major disadvantage of capillary gel electrophoresis is the short capillary lifetime and thus a reduced reproducibility over a long period of time. An alternative to gel-filled capillaries is to use semidilute or dilute polymer solutions for polynucleotide separation [2–7]. Separations of RNA are used for the analysis of RNA mass, studies of conformation, and in RNA hybridization techniques [8, 9]. Separations in capillaries have been reported for both small (transfer and 5S ribosomal RNA, 80 and 120 nucleotides (nt), respectively) and large RNA (281-6583 nt RNA ladder and bacterial and eukaryotic ribosomal RNA) [10–15]. In our study we focus on the mechanism of electrophoretic migration of RNA molecules of different sizes (281-6583 nt).

Several models have been developed to describe the separation of DNA molecules in polymer solutions [16–29], most recently reviewed by Viovy, Slater and Albarghouthi [30–32]. Below the entanglement threshold c^* (where no network is formed between the sieving molecules) separation is thought to occur by the transient entanglement mechanism [26, 27, 33]. In this case, the nucleic acid goes through a cycle of collision with one or more polymer molecules followed by slow escape from the polymers. In the past few years, video microscopy has confirmed that the DNA molecule becomes hooked to a polymer molecule, extends, goes through a U-shape formation leading to a slow disentanglement, and finally collapses to a random coil [20, 22, 24, 34].

In semidilute solutions, *i.e.*, above the entanglement threshold and in the presence of a flexible matrix network, the separation of small DNA oligonucleotides proceeds by a mechanism related to Ogston sieving [35]. This model relies purely on geometrical arguments based on the assumption that the media is a sieve containing many pores. The polynucleotide then has a mobility that is directly dependent on the concentration of the sieving polymer:

$$\mu/\mu_0 = e^{-Kc} \quad (1)$$

μ is the mobility of the nucleic acid, μ_0 is the mobility in free solution, K is the retardation coefficient and c is the polymer concentration. Since this model was developed for rigid matrices and globular objects, it cannot be used to fully describe the electrophoretic migration of small biopolymers in semidilute solutions.

For larger DNA oligonucleotides (for which the radius of gyration, R_g, is larger then the average pore size, ξ) in a semidilute solution, electrophoretic separation proceeds by segmental motion [30]. The reptation model was originally developed for cross-linked gels, but the theory has been further extended to semidilute polymer solutions [30, 36]. Two limits of electrophoretic migration are known for segmental motion: (i) for pore sizes ξ, larger than the Kuhn length b_D, and (ii) for ξ smaller than b_D, which is the

Correspondence: Dr. Michael D. Morris, Dr. Nils G. Walter, Department of Chemistry, University of Michigan, Ann Arbor, MI 48109-1055, USA
E-mail: mdmorris@umich.edu
nwalter@umich.edu
Fax: +734-615-1293

Abbreviations: FWHM, full width at half maximum; **HEC**, hydroxyethylcellulose; **nt**, nucleotide; **TBE**, Tris-boric acid-EDTA buffer

case of tightly composed sieving polymer solution. In the first case, when a DNA molecule is smaller than a critical size N^*, the mobility of the polynucleotide is dependent on the chain length and good separations can be obtained (reptation without orientation). For DNA larger than N^*, the mobility becomes dependent only on the applied electric field and not on the size of the polynucleotides (reptation with orientation). This leads to loss of separation capability. However, recently Heller [36] showed that, for entangled polymer solutions, size separation still occurs, but with decreased efficiency.

The above models were developed for DNA separation in cross-linked matrices. However, in entangled solutions the pores have a finite lifetime, *i.e.*, the channels created by the polymer chains shift due to interactions with the surrounding polymers. As a result, DNA migrates by two different processes: through its own entanglements and through the entanglements of the matrix itself. This phenomenon has been described as constraint release (CR) [37]. If the mobility due to CR is higher than the mobility of the DNA migration itself, the separation fails.

In this paper, we present a study of the electrophoretic separation of RNA in dilute and semidilute polymer matrices. RNA molecules are single-stranded oligonucleotide chains with self-complementary regions giving rise to secondary and tertiary structures. In a study by Skeidsvoll and Ueland [13], it was shown that, for small and medium sized ribonucleotides, the separation may proceed by one mechanism (reflected in a straight line of migration time *vs.* RNA chain length). However, this investigation did not describe the electrophoretic migration of RNA longer than 2000 nt. In our study, we present the effects of urea denaturant to higher order structures of RNA of up to 6583 nt in length. In addition, polymer size and concentration dependence of mobility are investigated and the results are then compared to the models described above. Through such a study, valuable mechanistic information is obtained.

2 Materials and methods

The CE apparatus has been described elsewhere [5]. Briefly, a high-voltage power supply (Glassman Inc., Whitehouse Station, NJ, USA) was used to provide electrophoresis voltage. Detection was by a UV absorbance detector (Thermo Separation Products, Riviera Beach, FL, USA) at 260 nm. The whole separation system was placed in a Plexiglas box for operator safety. The applied voltage and data collection were controlled by a personal computer running with LabVIEW (National Instruments, Austin, TX, USA). Data were analyzed using GRAMS (Galactic Industries Corporation, Salem, NH, USA). Separations were performed in 50 μm ID, 365 μm OD fused-silica capillaries (Polymicro Technologies, Phoenix, AZ, USA) coated with polyacrylamide to minimize electroosmosis [38]. The capillary length used was 26.2 cm with an effective length of 21.5 cm. Hydroxyethylcellulose (HEC) was used as the separation polymer. Four different sizes of HEC were used in our study: M_r = 24 000–27 000 and M_r = 90 000–105 000 from Polysciences (Warrington, PA, USA) and M_r = 63 500 and M_r = 438 000 from Aqualon (Wilmington, DE, USA). Concentrations ranged from 0.0005 to 3% w/w in 1 × TBE (89 mM Tris, 89 mM boric acid, 2 mM EDTA; all components from Fisher Scientific, Fair Lawn, NJ, USA), 4 M urea (Sigma, St. Louis, MO, USA). The polymer solutions were stirred for 24 h to provide complete solvation of the polymer. Viscosities were measured with a falling ball viscosimeter (Cole-Parmer, Vernon Hills, IL, USA). The results were used for calculation of the overlap concentration, c^*, according to the method described by Barron *et al.* [6]. Viscosity measurements as a function of polymer concentration were used for determining c^*. The specific viscosity as a function of polymer concentration on a logarithmic scale is composed of two linear regions with different slopes. The point of intersection represents the entanglement threshold for a given polymer chain length. The whole region between the linear parts is the entanglement threshold range. A single-stranded RNA size marker (with RNAs: 281, 623, 955, 1383, 1908, 2604, 3638, 4981, 6583 nt) was purchased from Promega (Madison, WI, USA). Stock solutions were diluted to 100 μg/mL in 1 × TBE. For denaturation of the RNA, urea was added to the same concentration as in the running buffer. Injections were performed electrokinetically at 40–120 V/cm for 10 s, depending on the concentration of HEC. CE was performed in 1 × TBE containing different concentrations of sieving polymer. Urea concentrations ranging from 0 to 7.2 M were used for denaturation of the RNA molecules. The capillaries were filled with separation buffer using a vacuum pump for 2 min. All CE studies were performed with injection at the cathode and detection close to the anode. RNA electrophoretic mobility dominated the minimized electroosmotic flow and the total migration was from the cathode to the anode. All separations were performed at 26°C. Between runs, the capillaries were flushed for 1 min with 1 × TBE. At high concentrations of polymer (solution viscosity above 15 cP) TBE flushing was extended to 3 min in order to remove all HEC solution from the capillary.

3 Results and discussion

3.1 Entanglement threshold calculation

The entanglement threshold c^* is the concentration above which the polymer molecules start to interact with each other and form a flexible network. The entanglement

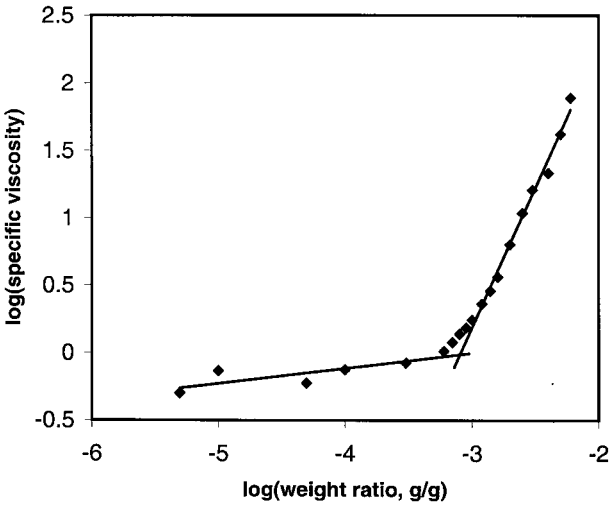

Figure 1. Dependence of specific viscosity on polymer concentration. Data shown for HEC, M_r = 438 000. The region between the straight lines represents the entanglement threshold range.

threshold range was determined for the four sizes of HEC used. Figure 1 is an example of the plot used for the determination of the entanglement threshold range for the HEC with M_r = 438 000. From the graph it can be observed that the change from freely moving polymers to a flexible network occurs at a narrow concentration range, 0.07–0.1 weight %. This range is due to the polydispersity of the polymer. The data for all sizes of polymers is summarized in Table 1. The slopes of viscosity *vs.* concentration above the entanglement threshold are the same for all four polymer sizes. This result is expected: after the polymer chains overlap with each other, the pore size no longer depends on the molecular weight of the polymer but only on the concentration of monomeric units in solution.

Table 1. Entanglement threshold for different chain lengths of HEC in 1 × TBE, 4 M urea

HEC M_r	Entanglement range (%HEC)	Entanglement threshold (%HEC)	Entanglement threshold (%HEC) from [6]
24 000–27 000	0.8–1.6	1.0	1.8
63 500	0.2–0.5	0.25	0.68
90 000–105 000	0.1–0.3	0.14	0.37
438 000	0.07–0.1	0.08	0.09

3.2 Electrophoretic separation of RNA

Figure 2 shows an example of the separation of the RNA size marker (281-6583 nt) using a c/c^* = 2.25 (HEC, M_r = 90 000–105 000). The separation was performed at 330 V/cm in 1 × TBE, 4 M urea. The first five peaks show high resolution, but above ~2000 nt the resolution decreases. Higher resolution for the larger RNA molecules was obtained using M_r = 438 000 HEC (data not shown). However, in this case a decrease in the resolution for the smaller members of the RNA ladder was observed.

3.3 Effect of denaturing agent on RNA separation

We studied the effect of urea concentration on RNA separation. A number of experiments were performed in which the concentration of urea was varied from 0 to 7.2 M. Figure 3 shows the dependence of RNA electrophoretic mobility on urea concentration. The mobility gradually

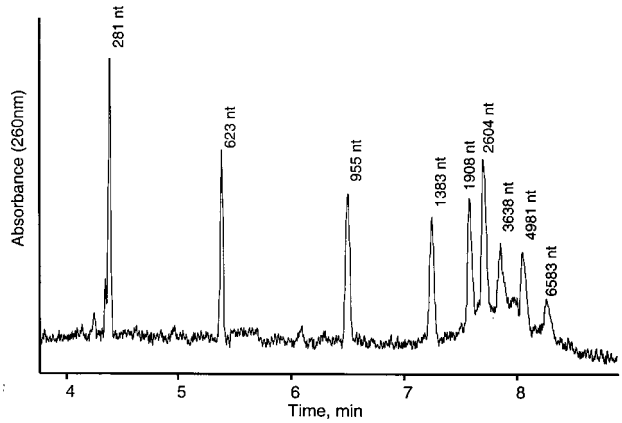

Figure 2. Electropherogram showing a separation of RNA marker (281–6583 nt). The sample was denatured in 4 M urea, 1 × TBE, injected at 80 V/cm and separated in a coated capillary filled with c/c^* = 2.25 (HEC, M_r = 90 000–105 000), 4 M urea, 1 × TBE, at 330 V/cm. Detection was UV absorbance at 260 nm.

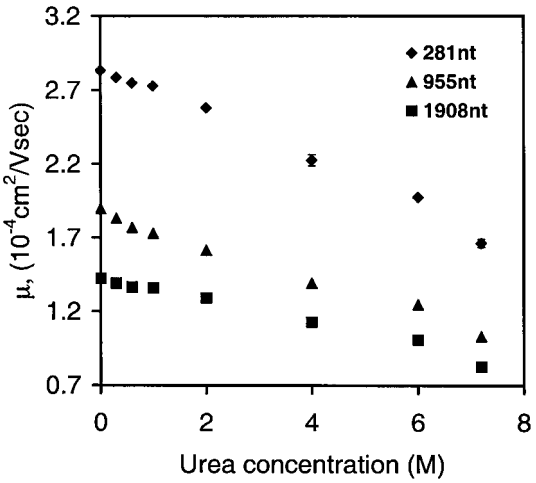

Figure 3. Dependence of RNA mobility on urea concentration. Data shown for c/c^* = 5.9 (HEC, M_r = 438 000), 1 × TBE, injected at 75 V/cm for 10 s, separation at 260 V/cm.

decreased with increasing urea concentration. The efficiency of the separation remained constant between 2 and 7.2 M urea. For comparison, the free solution mobility dependence on urea concentration is shown in Table 2.

The full width at half maximum (FWHM) can be used to study the presence of multiple conformations of plasmid DNA, *i.e.*, confirming of the presence of different topoisomers [39, 40]. We studied the dependence of FWHM adjusted to the electrophoretic mobility of the members of the RNA marker on the urea concentration (Fig. 4). Up to 2 M urea, RNAs larger than 2604 nt were not resolved and their separation failed. Our results for smaller RNAs demonstrate that the 281 nt and 623 nt long ones (latter not shown) had higher FWHM. The band widths of the 1383 nt and 1908 nt long RNAs (first one not shown) showed decrease of FWHM with increasing urea concentration, that were smaller than those for the short RNAs. The FWHM of the 955 nt long RNA remained almost constant up to 7.2 M urea.

Table 2. Free solution mobility of RNA marker at different urea concentrations

Urea concentration (M)	RNA mobility (10^{-4}cm^2/Vs)
0	5.06
1	5.06
2	5.00
3	4.74
4	4.32
5	4.08
6	3.78

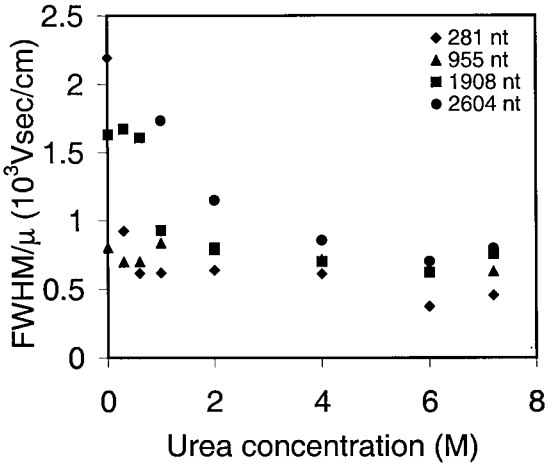

Figure 4. FWHM (adjusted to RNA mobility) as a function of urea concentration. Data shown for c/c^* = 5.9 (HEC, M_r = 438 000). Conditions as in Fig. 3.

The decrease of the band widths with increasing urea concentration is most probably a consequence of the melting of alternative secondary and tertiary structures. Broad bands are produced by the presence of rapidly interconverting conformations that are not resolved. The higher order structures of RNA are dependent not only on chain length but also on the nucleotide sequence. Therefore, it can be expected that two RNAs can have very different band widths, although they have the same or similar chain lengths. By the same argument, similar band widths can be obtained for different length RNAs as observed here. Above 2 M urea, denaturation is extensive and alternative secondary and tertiary structures are suppressed. Therefore, at high urea concentrations all RNA molecules migrate as narrow bands and the band widths depend weakly on chain length and sequence.

3.4 Mobility and RNA size

We investigated the mobility of RNA molecules in the presence of polymers of different chain length and concentration. Figure 5 shows the dependence of mobility on the RNA chain length. The electrophoretic migration of RNA below the entanglement threshold, *i.e.*, dilute solutions, fits for c/c^* = 0.6 (HEC, M_r = 24 000–27 000), c/c^* = 0.8 (HEC, M_r63 500), c/c^* = 0.7 (HEC, M_r = 90 000–105 000 and c/c^* = 0.4; 1.2 (HEC, M_r = 438 000) upper traces in A, B, C, D, proceeds by one mechanism, as a single linear relationship is observed for all sizes of HEC used. The

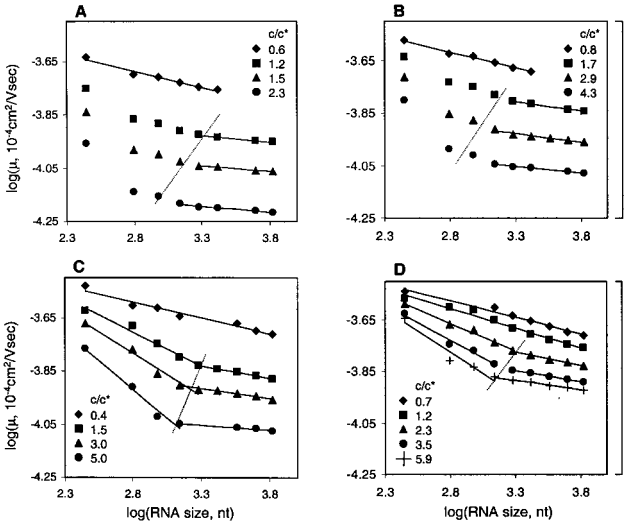

Figure 5. Dependence of electrophoretic mobility on RNA size, separated in HEC, 4 M urea, 1 × TBE. (A) M_r = 24 000–27 000. (B) M_r = 63 500, (C) M_r = 90 000–105 000, (D) M_r = 438 000. Conditions as in Fig. 2. The straight lines indicate linear regression fit. Dotted lines represent the critical chain length N^*.

resolution obtained at shorter polymer chains (M_r = 24 000–27 000 and M_r = 63 500) is reduced for RNA above 3600 nt in length and the bands start to overlap. The slopes for the regression fits shown in Fig. 5 are tabulated in Table 3. The average slope of the straight lines is –0.13. We have previously reported –0.08 slopes for long double stranded and –0.16 for supercoiled DNA in dilute polymer solutions [4]. The radius of gyration of a random coil scales as $1/N$ and the radius of gyration of an elastic rod scales as $1/N^{1/2}$ [41]. Using scaling arguments and electrophoretic data for double-stranded and supercoiled DNA, it was confirmed that ds-DNA migrates in random coil fashion and scDNA as an elastic rod [4]. The slope that we determined for RNA falls between the values for a scDNA (rod limit) and a dsDNA (random coil limit), although closer to the rod limit. This observation is not unexpected since RNA probably retains some secondary structure elements (*i.e.*, double-stranded regions) even under denaturing conditions, although probably only the most stable ones, limiting the number of alternative conformations. This may give RNA more rigidity than linear dsDNA, but less rigidity than supercoiled plasmids.

Table 3. Linear regression fit of the logarithmic plots of mobility as a function of RNA size

HEC M_r	c/c^*	Regime 1	Regime 2	Mode
24 000–27 000	0.6	–0.12		Dilute
	1.2	–0.11	–0.05	Semidilute
	1.5	–0.13	–0.04	Semidilute
	2.3	–0.12	–0.05	Semidilute
63 500	0.8	–0.12		Dilute
	1.7	–0.15	–0.07	Semidilute
	2.9	–0.16	–0.07	Semidilute
	4.3	–0.15	–0.05	Semidilute
90 000–105 000	0.4	–0.12		Dilute
	1.5	–0.26	–0.09	Semidilute
	3.0	–0.32	–0.07	Semidilute
	5.0	–0.43	–0.04	Semidilute
438 000	0.7	–0.13		Dilute
	1.2	–0.15		Dilute
	2.3	–0.21	–0.11	Semidilute
	3.5	–0.27	–0.08	Semidilute
	5.9	–0.33	–0.07	Semidilute

For semidilute polymer systems, above the entanglement threshold, we observe two mobility regimes in the electrophoretic motion of RNA (Fig. 5). Below the RNA critical length (see dotted lines), the separation efficiency is high. Good separations can be obtained for medium-sized polyribonucleotides (200–2000 nt long RNA) using long sieving polymer molecules (HEC, M_r = 90 000–105 000 and M_r = 438 000 Fig. 4C, D). For short polymer chains (HEC, M_r = 24 000–27 000 and M_r = 63 500, Fig. 4A, B), the region between the two regimes is extended and high resolution can be obtained only for RNAs shorter than 600 nt. In the second regime, for RNA longer than the critical size, the mobility *vs.* size slope decreases, but separation is still possible, although with a loss of resolving power.

The data do not completely agree with the theoretical predictions by Viovy *et al.* [30, 37] that the separation capability will be lost. This is probably due to the fact that these earlier theoretical predictions were made for classical gel electrophoresis while we are using semidilute polymer solutions. In addition, the theory was developed for single-stranded DNA and dsDNA, and as was described in Section 3.3, RNA can still have some secondary structure remaining even under denaturing conditions. Therefore, the behavior of RNA in electric fields is to some extent different from DNA undergoing electrophoretic migration. The limiting case developed for DNA migration in semidilute polymer solutions may not completely describe RNA migration in similar solutions.

Another interesting feature in Fig. 5 is that the critical size (dotted lines) shifts to shorter RNA lengths as the polymer concentration is increased. In addition, an increase in resolution is observed for RNAs smaller than the critical size. These tendencies are observed for all HEC chain lengths. We interpret this result as a decrease in pore size as the concentration of polymer increases. As mentioned above (Section 3.1), the pore size depends only on the concentration of polymer segments but not on the chain length.

3.5 Mobility and polymer concentration

Figure 6 shows the dependence of the RNA mobility on the concentration of HEC. The example shown is for HEC with M_r = 438 000. The first break, at c/c^* = 1, shows

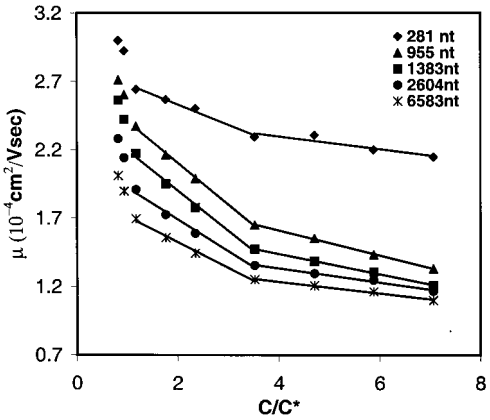

Figure 6. Dependence of RNA electrophoretic mobility on polymer concentration. Data shown for HEC, M_r = 438 000. Conditions as in Fig. 2. Straight lines are just guide for the eye.

the change in viscosity of the solution, *i.e.*, reaching the entanglement threshold range. This slope change indicates the point at which RNA migration changes from transient entanglements with the free polymer molecules to more frequent interactions with the polymer and possible secondary entanglements. A second break is observed in Fig. 6 at $\sim c/c^* = 3.5$. The change in the behavior of the polymer can be attributed to a stiffer network. In this regime, the migrating RNA can no longer drag the polymer chains with itself and thus disrupt the sieving network. This result shows that RNA electrophoretic migration in semidilute polymer solutions proceeds by a complicated mechanism that cannot be described by a single existing model. Further investigations into RNA electrophoresis are underway in our laboratories.

4 Concluding remarks

In this paper, we present a study of single-stranded RNA electrophoretic migration and separation in polymer solutions. A study of the denaturing agent concentration indicates the importance of melting alternative higher-order structures for the resolution of RNA. In dilute polymer solutions in the presence of 4 M urea as a denaturant, RNA migrates similarly to a random coil with some stable secondary structures formed making the molecule somewhat stiff so that it acts partially as a rigid rod. In semidilute solutions, RNA electrophoresis proceeds by segmental motion. Our data also reveals a complicated migration dependence on polymer concentration. The results presented here should help optimize RNA separation and also provide information about the intriguing mechanisms of RNA migration in an electric field.

We gratefully acknowledge support from the National Institutes of Health through Grant R01-GM37006 to M.D.M. and from The University of Michigan through funds to N.G.W.

Received December 14, 2000

5 References

[1] Landers, J. P., *Handbook of Capillary Electrophoresis*, CRC Press, Boca Raton, FL 1997.

[2] De Carmejane, O., Schwinefus, J. J., Wang, S. C., Morris, M. D., *J. Chromatogr. A* 1999, *849*, 267–276.

[3] Oana, H., Hammond, R. W., Schwinefus, J. J., Wang, S. C., Doi, M., Morris, M. D., *Anal. Chem.* 1998, *70*, 574–579.

[4] Hammond, R. W., Oana, H., Schwinefus, J. J., Bonadio, J., Levy, R. J., Morris, M. D., *Anal. Chem.* 1997, *69*, 1192–1196.

[5] Kirn, Y., Morris, M. D., *Anal. Chem.* 1994, *66*, 3081–3085.

[6] Barron, A. E., Soane, D. S., Blanch, H. W., *J. Chromatogr.* 1993, *652*, 3–16.

[7] Barron, A. E., Sunada, W. M., Blanch, H. W., *Electrophoresis* 1995, *16*, 64–74.

[8] Melton, D. A., Krieg, P. A., Rebagliatti, M. R., Maniatis, T., Zinn, K., Green, M. R., *Nucleic Acids Res.* 1984, *12*, 7035–7056.

[9] Thomas, P. S., *Proc. Natl. Acad. Sci. USA* 1980, *77*, 5201–5205.

[10] Cellai, L., Onori, A. M., Desiderio, C., Fanali, S., *Electrophoresis* 1998, *19*, 3160–3165.

[11] Saevels, J., Van Schepdael, A., Hoogmartens, J., *Anal. Biochem.* 1999, *266*, 93–101.

[12] Ogura, M., Agata, Y., Watanabe, K., Mccormick, R. M., Hamaguchi, Y., Aso, Y., Mitsuhashi, M., *Clin. Chem.* 1998, *44*, 2249–2255.

[13] Skeidsvoll, J., Ueland, P. M., *Electrophoresis* 1996, *17*, 1512–1517.

[14] Katsivela, E., Hofle, M. G., *J. Chromatogr. A* 1995, *777*, 91–103.

[15] Katsivela, E., Hofle, M. G., *J. Chromatogr. A* 1995, *700*, 125–136.

[16] Shi, X. L., Hammond, R. W., Morris, M. D., *Anal. Chem.* 1995, *67*, 3219–3222.

[17] Ueda, M., Yoshikawa, K., Doi, M., *Polymer J.* 1999, *31*, 637–644.

[18] Ueda, M., Yoshikawa, K., Doi, M., *Polymer J.* 1997, *29*, 1040–1043.

[19] Oana, H., Masubuchi, Y., Matsumoto, M., Doi, M., Yoshikawa, K., *J. Polymer Polymer Phys.* 1996, *34*, 1105–1111.

[20] Oana, H., Masubuchi, Y., Matsumoto, M., Doi, M., Matsuzawa, Y., Yoshikawa, K., *Macromolecules* 1994, *27*, 6061–6067.

[21] Minagawa, K., Matsuzawa, Y., Yoshikawa, K., Khokhlov, A. R., Doi, M., *Biopolymers* 1994, *34*, 555–558.

[22] Schwartz, D. C., Koval, M., *Nature* 1989, *338*, 520–522.

[23] Masubuchi, Y., Oana, H., Ono, K., Matsumoto, M., Doi, M., Minagawa, K., Matsuzawa, Y., Yoshikawa, K., *Macromolecules* 1993, *26*, 5269–5270.

[24] Smith, S. B., Aldridge, P. K., Callis, J. B., *Science* 1989, *243*, 203–206.

[25] Starodoubtsev, S. G., Yoshikawa, K., *Langmuir* 1998, *14*, 214–217.

[26] Hubert, S. J., Slater, G. W., *Electrophoresis* 1995, *16*, 2137–2142.

[27] Hubert, S. J., Slater, G. W., Viovy, J. L., *Macromolecules* 1996, *29*, 1006–1009.

[28] Murayama, H., Yoshikawa, K., *J. Phys. Chem. B* 1999, *103*, 10517–10523.

[29] Shi, X., Hammond, R. W., Morris, M. D., *Anal. Chem.* 1995, *67*, 1132–1138.

[30] Viovy, J. L., *Rev. Mod. Phys.* 2000, *72*, 813–872.

[31] Slater, G. W., Desruisseaux, C., Hubert, S. J., Mercier, J. F., Labrie, J., Boileau, J., Tessier, F., Pepin, M. P., *Electrophoresis* 2000, *21*, 3873–3887.

[32] Albargheuthi, M. N., Barron, A. E., *Electrophoresis* 2000, *21*, 4096–4111.

[33] Barron, A. E., Blanch, H. W., Soane, D. S., *Electrophoresis* 1994, *15*, 597–615.

[34] Shaffer, J. S., *Macromolecules* 1996, *29*, 1010–1013.

[35] Ogston, A. G., *Trans. Far. Soc.* 1958, *54*, 1754–1757.

[36] Heller, C., *Electrophoresis* 1999, *20*, 1962–1977.

[37] Viovy, J.-L., Duke, T., *Electrophoresis* 1993, *14*, 322–329.

[38] Hjertén, S. J., *J. Chromatogr.* 1985, *347*, 191–198.

[39] Rill, R. L., Locke, B. R., Liu, Y. J., Van Winkle, D. H., *Proc. Natl. Acad. Sci. USA* 1998, *95*, 1534–1539.

[40] De Carmejane, O., Schwinefus, J. J., Morris, M. D., *Proc. SPIE* 1999, *3602*, 346–354.

[41] Cantor, C. R., Schimmel, P. R., *Biophysical Chemistry*, W. H. Freeman and Co., San Francisco, CA 1980, Vol. 3.